# FLOW OVER CIRCULAR CYLINDER SIMULATIONS USING FOURIER PSEUDO-SPECTRAL METHOD WITH IMMERSED BOUNDARY

**Felipe Pamplona Mariano, fpmariano@mecanica.ufu.br**
**Leonardo de Queiroz Moreira, lqmoreira@mecanica.ufu.br**
**Aristeu da Silveira Neto, aristeus@mecanica.ufu.br**
Universidade Federal de Uberlândia - UFU
Faculdade de Engenharia Mecânica - FEMEC
Laboratório de Mecânica dos Fluidos - MFLab
Av: João Naves de Ávila, 2121
Campus Santa Mônica Bl: 5P - sala: 304
CEP: 38400-902 Uberlândia-MG-Brasil

**Abstract.** *The Immersed Boundary Method (IB) has been widely used in Computational Fluids Dynamic (CFD) in order to simulate flows over complex geometries. IB represents the boundary conditions through a force field imposed at Navier-Stokes equations. Nevertheless, generally, it presents low accuracy and low convergence order. Aiming to solve this restriction, a new methodology is proposed at the present work, by using the Pseudo-Spectral Fourier Method. This method provides an excellent numerical accuracy, and with the development of the Fast Fourier Transform algorithm (FFT), it presents a low computational cost in comparison with another high-order methods. Another important issue is the projection method of the pressure term. In the Fourier space, this procedure does not require a Poisson solver, which is usually the most computational onerous part in classical methodologies. In order to validate the new methodology it was proposed two problems simulations. The first is a Green-Taylor Vortex, which has analytical solution and capability of show the accuracy and high order convergence. The second is flow around a circular cylinder that is a classical problem of CFD.*

***Keywords****: Computational Fluids Dynamic, Green-Taylor Vortex, Circular Cylinder, Fourier Pseudo-Spectral Method, Immersed Boundary Method.*

## 1. INTRODUCTION

Phenomena involving aeroacustic, transition to turbulence and combustion are problems that modern engineering aim to understand, among other manners, by using techniques of Computational Fluids Dynamics (CFD). In case of the aeroacustic is important to use a method that captures the sound pressure waves. In phenomena involving transition to turbulence is necessary to study small instabilities that become the flows turbulent. In combustion, there are processes that involve small edges of turbulent flow. In these problems CFD uses methods of high order accuracy to obtain results to analyse which really represent the physics phenomena mentioned.

High order methods provide an excellent accuracy. For example: methods of high order finite differences and compact schemes, but, on the other hand, they have disadvantaged of computational expensive cost in comparison to conventional methodologies. The advent of spectral methods become possible joining high accuracy with low computational cost. This low cost is given by the Fast Fourier Transformed (FFT), since the cost of a problem resolution with finite differences is the order of $O(N^2)$, where $N$ is the number of the grid points, the cost of the FFT is of $O(N\log_2 N)$ (Canuto *et al.*, 2006). In addition, it was also developed the projection method (Canuto *et al.*, 2007), which disentails pressure field of Navier-Stokes equation calculates in the spectral space. Using the projection process is not necessary to calculate the Poisson equation, as it is has been done by conventional methodologies. Normally, solving this equation is the most expensive part of a CFD code. The disadvantage of the spectral methodology is the difficulty to work with complex geometries and boundary conditions.

One of the most practical methodologies to work with complex geometries is the Immersed Boundary (IB) (Peskin, 1972). It is distinguished by the imposition of a term source, which has the role of a body force imposed in the Navier-Stokes equation to represent a virtual immersed body in the flow (Goldstein *et al*, 1993), and this facilitates to represent any geometry, whether it is complex or in movement.

A new methodology, presented in this paper, works with Fourier pseudo-spectral method connected in immersed boundary method. It is proposed to simulate flows with non-periodic boundary conditions make using of the term source of immersed boundary. On the other hand, the accuracy of immersed boundary is improved with smooth solution problems.

First, it will be demonstrated the transformation of Navier-Stokes equations for Fourier spectral space, as well as the imposition of the source term. In the second part, details of numerical implementation of computational code developed will be demonstrated. Finally, the results of Taylor-Green Vortex flow will be shown high order accuracy in immersed interface and the simulations of flow over a circular cylinder, which is a non-periodic problem solved by the Fourier spectral method, where the boundary conditions has been imposed through of the force field of the immersed boundary.

## 2. MATHEMATICAL MODELING

In this session will be presented the mathematical model of immersed boundary method based in Multi-Direct Forcing proposed by Wang *et al*. (2007), after that, the equations that govern the problem will be transformed for the Fourier spectral space using the properties of discrete Fourier transformed and, finally, the methodology proposed by this paper will be presented connecting the two methodologies.

### 2.1. Mathematic model for the fluid

The flow is governed by conservation momentum equation (Eq. 1) and the continuity equation (Eq. 2). The information of the fluid/solid interface (domain Γ) is passed to the eulerian domain (Ω) for addition of the term source to Navier-Stokes equations. This term plays a role of a body force that represents the boundary conditions of the immersed geometry (Goldstein *et al*, 1993). The equations that govern the problem are presented in theirs tensorial form:

$$\frac{\partial u_l}{\partial t}+\frac{\partial (u_l u_j)}{\partial x_j}=-\frac{\partial p}{\partial x_l}+\nu\frac{\partial^2 u_l}{\partial x_j \partial x_j}+f_l \tag{1}$$

$$\frac{\partial u_j}{\partial x_j}=0 \tag{2}$$

where $\frac{\partial p}{\partial x_l}=\frac{1}{\rho}\frac{\partial p^*}{\partial x_l}$; $p^*$ is the static pressure in [$N/m^2$]; $u_l$ is the velocity in $l$ direction in [$m/s$]; $f_l=\frac{f_l^*}{\rho}$; $f_l^*$ is the term source in [$N/m^3$]; $\rho$ is the density; $\nu$ is the cinematic viscosity in [$m^2/s$]; $x_l$ is the spatial component ($x,y$) in [$m$] and $t$ is the time in [$s$]. The initial condition is any velocity field that satisfies the continuity equation.

The source term is defined in all domain Ω, but presents different values from zeros only in the points that coincide with the immersed geometry, enabling that the eulerian field perceives the presence of solid interface (Enriquez-Remigio and Silveira Neto, 2007).

$$f_l(\vec{x},t)=\begin{cases}F_l(\vec{x}_k,t) & \text{if } \vec{x}=\vec{x}_k\\ 0 & \text{if } \vec{x}\neq\vec{x}_k\end{cases} \tag{3}$$

where $\vec{x}$ is the position of the particle in the fluid and $\vec{x}_k$ is the position of a point in solid interface (Fig. 1).

The boundary conditions are periodic in all directions in eulerian domain $\Omega_B$, as showed in Fig. 1, it is necessary due pseudo-spectral method properties. The boundary condition of the problem simulated is imposed by direct forcing methodology in $\Gamma_{BC}$, and also the boundary conditions of bodies immersed in flow $\Gamma_i$.

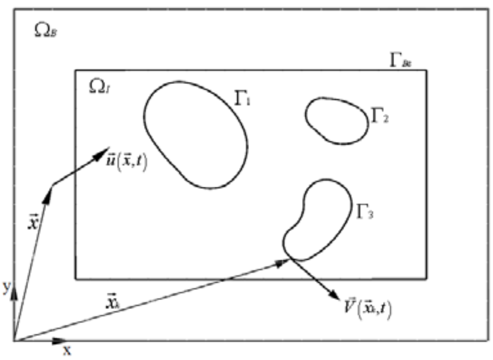


Figure 1. Schematically representation of eulerian and lagrangian domain.

Using Eq. (3) can be concluded that the field $f_l(\vec{x},t)$ is discontinuous, which can be numerically solved only when there are coincidence between the points that compose the interface domain with the compose the fluid domain. In cases there is no coincidence between these points, very frequently in the complex geometries, it is necessary to distribute the function $f_l\left(\vec{x},t\right)$ on its neighborhoods. Just by calculating the lagrangian force field $F_l\left(\vec{x}_k,t\right)$, it can be distributed and thus, transmitted the information geometry presence for eulerian domain, these functions can be found in Griffith and Peskin, (2005).

### 2.2. Mathematic model for the immersed interface

The lagrangian force field, in this study, is calculated by direct forcing methodology, which was proposed by Uhlmann (2005). One of the characteristics of this model is that is not necessary using ad-hoc constants and allows the modeling non-slip condition on immersed interface. The lagrangian force $F_l\left(\vec{x}_k,t\right)$ is available by momentum conservation equation over a fluid particle that is joined in the fluid-solid interface, Eq. (4):

$$F_l\left(\vec{x}_k,t\right)=\frac{\partial u_l}{\partial t}\left(\vec{x}_k,t\right)+\frac{\partial}{\partial x_j}(u_lu_j)\left(\vec{x}_k,t\right)+\frac{\partial p}{\partial x_l}\left(\vec{x}_k,t\right)-\nu\frac{\partial^2 u_l}{\partial x_j\partial x_j}\left(\vec{x}_k,t\right) \tag{4}$$

The values of $u_l\left(\vec{x}_k,t\right)$ and $p\left(\vec{x}_k,t\right)$ are done by interpolation of velocities and pressure, respectively, of eulerian points near the immersed interface. For lagrangian point $x_k$ at the immersed boundary, we have:

$$F_l\left(\vec{X}_k,t\right)=\frac{u_l\left(\vec{x}_k,t+\Delta t\right)-u_l^*\left(\vec{x}_k,t\right)+u_l^*\left(\vec{x}_k,t\right)-u_l\left(\vec{x}_k,t\right)}{\Delta t}+RHS_l\left(\vec{x}_k,t\right) \tag{5}$$

where $u^*$ is a temporary parameter (Wang, et al., 2007), $\Delta t$ is the time step and $RHS_l\left(\vec{x}_k,t\right)=\frac{\partial}{\partial x_j}(u_lu_j)\left(\vec{x}_k,t\right)+\frac{\partial p}{\partial x_l}\left(\vec{x}_k,t\right)-\nu\frac{\partial^2 u_l}{\partial x_j\partial x_j}\left(\vec{x}_k,t\right)$. The Eq. (5) is solved by Eqs. (6) and (7) at same time step:

$$\frac{u_l^*\left(\vec{x}_k,t\right)-u_l\left(\vec{x}_k,t\right)}{\Delta t}+RHS_l\left(\vec{x}_k,t\right)=0 \tag{6}$$

$$F_l\left(\vec{x}_k,t\right)=\frac{u\left(\vec{x}_k,t+\Delta t\right)-u_l^*\left(\vec{x}_k,t\right)}{\Delta t} \tag{7}$$

where $u\left(\vec{x}_k,t+\Delta t\right)=U_{FI}$ is the immersed boundary velocity, normally known.

Eq. (6) is solved at eulerian domain at Fourier spectral space, i.e. the solution of Eq. (1) with $f_l=0$. $u_l^*\left(\vec{x},t\right)$ is interpolated for lagrangian domain, became $u_l^*\left(\vec{x}_k,t\right)$ and it is computed on Eq. (7). Then $F_l\left(\vec{x}_k,t\right)$ is smeared for eulerian mesh. Finally, the velocity is update by Eq. (8):

$$u_l\left(\vec{x},t+\Delta t\right)=u_l^*\left(\vec{x},t\right)+\Delta t.f_l \tag{8}$$

### 2.3 Fourier Transforms

By defining the equations that govern the flow through immersed boundary method, the next step is transforming them to the Fourier spectral space. It applies the Fourier transform in the continuity Eq. (2):

$$ik_j\hat{u}_j=0 \tag{9}$$

According to analytic geometry the scalar product between two vectors is null, if both are just orthogonal. Therefore, from Eq. (9), the wave number vector $k_j$ is orthogonal to transform velocity $\hat{u}_j$. The plane of divergent free (plane π) is defining, perpendicular to wave number vector $\vec{k}$ and thus, transformed velocity vector $\hat{\vec{u}}\left(\vec{k},t\right)$ belongs to the plane $\pi$.

Now applying the Fourier transform in the momentum Eq. (6):

$$\frac{\partial \hat{u}_l^*}{\partial t} + ik_j \widehat{u_l^* u_j^*} = -ik_l \hat{p} - \nu k^2 \hat{u}_l^* \tag{10}$$

where $k^2$ is the square norm of wave number vector, i.e. $k^2=k_jk_j$.

In agreement of plane π definition, each one of the terms of Eq. (10) assume a position related to it: the transient term $\frac{\partial \hat{u}_l^*}{\partial t}$ and the viscous term $\nu k^2 \hat{u}_l^*$ belong to the plane π. The gradient pressure term is perpendicular to plane π, and non-linear, $ik_j \widehat{u_l^* u_j^*}$, a priori, it is not known in which position it can be found in relation to plane π. By joining the terms of Eq. (10) and observing the definition of plane π, we have found that:

$$\underbrace{\left[\frac{\partial \hat{u}_l^*}{\partial t} + \nu k^2 \hat{u}_l^*\right]}_{\in \pi} + \left[ik_j \widehat{u_l^* u_j^*} + ik_l \hat{p}\right] = 0 \quad \Rightarrow \quad \underbrace{\left[ik_j \widehat{u_l^* u_j^*} + ik_l \hat{p}\right]}_{\in \pi} \tag{11}$$

To close Eq. (11), is needed that the non-linear and the force field terms are over plane π. For that, it is utilized projection tensor definition (Canuto *et al.*, 2007), which projects any vector over it. Therefore, applying this definition on the right hand side of the sum done in Eq. (11):

$$\left[ik_j \widehat{u_j^* u_l^*} + ik_l \hat{p}\right] = \wp_{lm}\left[ik_j \widehat{u_m^* u_l^*}\right] \tag{12}$$

The parcel of the gradient pressure field is orthogonal to plane π, then, it is zero after to be projected, disentailing from calculates of Navier-Stokes equations in the spectral space. The pressure field can be recovered at the pos-processing manipulating Eq. (12) (Mariano, 2007).

Other important point is non-linear term, in which appears the product of transformed functions, in agreement with Fourier transformed properties, this operation is a convolution product and its solution is given by convolution integral, this is solved by pseudo-spectral Fourier method (Canuto *et al.*, 2007). Therefore the momentum equation in the Fourier space, using the method of the projection, assumes the following form:

$$\frac{\partial \hat{u}_l^*(\vec{k},t)}{\partial t} + \nu k^2 \hat{u}_l^*(\vec{k},t) = -ik_j \wp_{lm} \int_{\vec{k}=\vec{r}+\vec{s}} \hat{u}_m^*(\vec{r},t)\, \hat{u}_l^*(\vec{k}-\vec{r},t)\, d\vec{r} \tag{13}$$

Non-linear term can be handed by different forms: advective, divergent, skew-symmetric, or rotational (Canuto *et al.*, 2006), in spite of being the same mathematically, they present different properties when discretized. The skew-symmetric form is more stable and present best results, but is twice more onerous that the rotational form. However this inconvenience can be solved using the alternate skew-symmetric form, it is consisting in alternate between the advective and divergent forms in each time step (Souza, 2005), it is proceeding adopted for this paper.

For all types of handing the non-linear term is necessary solve the convolution integral, but its numerical solution is computational expensive, then the pseudo-spectral method is used, i.e. calculates the velocity product in the physical space and transforms this product for the spectral space.

When solved numerically the Navier-Stokes equations with the Fourier spectral method using the Discrete Fourier Transform (DFT), which is define by Briggs and Henson (1995):

$$\hat{f}_k = \sum_{n=-N/2+1}^{N/2} f_n e^{\frac{-i2\pi kn}{N}} \tag{14}$$

when $k$ is wave number, $N$ is number of meshes points, $n$ get the position $x_n$ of collocation points ($x_n=n\Delta x$) and $i = \sqrt{-1}$.

The DFT restriction is periodic boundary conditions, by limiting the use of Fourier spectral transformed for CFD problems. The advantage is low computational cost gives by Fast Fourier Transform (FFT) (Cooley and Tukey, 1965), which solves the DFT (Eq. 12) of a way very efficiently, order $O(N\log_2 N)$. For systems with many collocation points, e.g. tridimensionals problems, the spectral method is very cheap when compared with another conventional high order methodologies. Two examples of use this method are simulations of periodic temporal jets and turbulence isotropic.

### 2.4. Proposed Methodology: IMERSPEC

The algorithm of methodology purposed is:

1) Solve the equation (12) in Fourier spectral space and obtain the temporal parameter $\hat{u}^*\left(\vec{k},t\right)$, using the low dispersion and low storage Runge-Kutta method proposed by Berland *et al.*, (2006) is used;

2) Use the Inverse Fast Fourier Transformer in $\hat{u}^*\left(\vec{k},t\right)$ and obtain $u^*\left(\vec{x},t\right)$ at physic space in the domain Ω;

3) Interpolate $u^*\left(\vec{x},t\right)$ for the lagrangian domain by cubic function proposed by Griffith and Peskin *et al.* 2005, and obtain $u^*\left(\vec{x}_k,t\right)$;

4) Calculate the lagrangian force, $F_l\left(\vec{x}_k,t\right)$, by Eq. 7.

5) Distribute the $F_l\left(\vec{x}_k,t\right)$ by cubic function proposed by Griffith and Peskin 2005, and obtain $f\left(\vec{x}_k,t\right)$ in eulerian domain;

6) Update the eulerian velocity, $u\left(\vec{x},t\right)$ by Eq. (8) and transformed it using FFT for spectral space, $\hat{u}^*\left(\vec{k},t\right)$, returned by step 1.

## 3. RESULTS

To validate the proposed methodology and developed code, two classical problems used in CFD were chosen. The first one is the Taylor-Green Vortex flow (Kin *et al.*,2001), which has an analytic solution to incompressible two-dimensional Navier-Stokes equations, with periodic boundary conditions. This case was useful in order to validate the developed pseudo-spectral code with the direct forcing. The second one, is the flow over a cylinder, which is a benchmark of CFD. This case allowed shows the solution of incompressible two-dimensional Navier-Stokes equations using Fourier pseudo-spectral method with non-periodic boundary conditions imposed by immersed boundary.

### 3.1. Taylor-Green Flows

The analytics equations to velocities components (*u* and v) and the pressure fields are given, conditioned to spatial coordinates (*x* and *y*) and time (*t*) (Canuto *et al.*, 2007):

$$u\left(x,y,t\right) = -U_\infty \cos(x).\sin(y).e^{-2t\nu} \quad (15)$$

$$\mathrm{v}\left(x,y,t\right) = U_\infty \sin(x).\cos(y).e^{-2t\nu} \quad (16)$$

$$p\left(x,y,t\right) = 0,25.U_\infty\left[\cos(2x)+\cos(2y)\right]e^{-4t\nu} \quad (17)$$

Where $U_\infty$ is the flow velocity amplitude in [*m/s*]. It is defined any geometry, which plays a role the immersed body in the flow. In this case is used a circle with diameter *D*=1*, where *D** is the diameter admensionalised by reference length, the diameter of one vortex *D=π* m. Therefore are defined two domains: eulerian and lagrangian, (Fig. 2). Can be observed that Eqs. (15) and (16) satisfy the continuity equation (Eq. 2), and the equation (17) allows the validation of the pressure field.

Several different cases were simulated refining the grid mesh and was taken the $L_2$ norm of components velocities and pressure, comparing to the analytical ($u_a$) and numerical ($u_N$) solutions (Eq. 18). The grid spacing is *h**, the Reynolds number is *Re=10*, $U_\infty = 1.0$ *m/s*, $\rho=1,0\ kg/m^3$ the domain length is $L_x^*=L_y^*=2$ and the time step is $\Delta t^* = \pi\ 10^{-4}$. The immersed boundary velocity ($U_{FI}$) is defined by Eqs. (15) and (16) in lagrangian positions ($\vec{x}_k$) and the lagrangian point space is *ds*=h**.

$$L_2 = \sqrt{\frac{1}{N_x}\frac{1}{N_y}\sum_{i=1}^{N_x}\sum_{j=1}^{N_y}\left\|u_N\left(x_i,y_j,t\right)-u_a\left(x_i,y_j,t\right)\right\|^2} \quad (18)$$

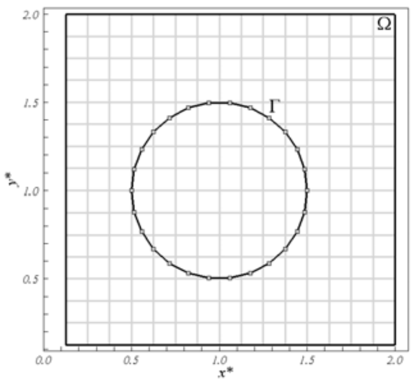


Figure 2. Sketch of eulerian (Ω) and lagrangian (Γ) domain.

The Fig. 3 presents the comparison between $L_2$ norm in function of grid refinement. The results show decaying of the fourth order for all variables. It is a good result in favor of immersed boundary methodology.

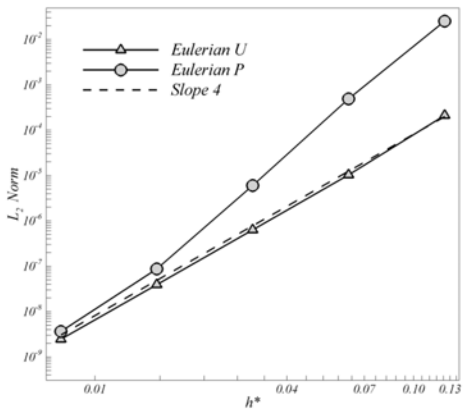


Figure 3. Comparison the $L_2$ norm in function of mesh spacing.

### 3.2 Flow over a cylinder

It is generate an inlet profile flow with velocity $U_\infty$ in [*m/s*], the flow cross the section of a circular cylinder (Fig. 2) and verify the drag (*Cd*) (Eq. 16) and lift (*Cl*) (Eq. 17) coefficients, these variables determine the forces that act on bodies immersed in flow, the drag coefficient determines the resistance force of the fluid on the immersed body, while the lift coefficient determines the force that there is in perpendicular direction to incoming flow, a interesting problem in aeronautical engineering is the optimization of airfoils, that consist in maximize the lift and minimized the drag of the airfoil profiles. Other parameter analyzed is the Strouhal number (*St*) (Eq. 18) which determines the non-dimensional vortex shedding, it is important to solve problems of fluid-structure, for example, pillars of bridges or aircraft wings, submitted to a flow, if the frequency of vortex shedding is close to the natural frequency is extremely damaging to this structures.

$$Cd = \frac{2\sum F_x}{\rho A_y U_\infty^2}, \tag{19}$$

$$Cl = \frac{2\sum F_y}{\rho A_x U_\infty^2}, \tag{20}$$

$$St = \frac{freq.D}{U_\infty}, \tag{21}$$

where: *Fx* and *Fy* are the forces estimated at each lagrangian point with Eq. (7) in [*N*]; *Ax* and *Ay* are projected frontal area in direction *x* and *y*, respectively . In bidimensional case these areas are given in [$m^2$] considered the perpendicular dimension of surface equal a unity, *D* is the characteristic diameter and *freq* is the vortex shedding frequency downstream of cylinder. The domain of all cases have been simulated is $6\pi \, x \, 2\pi$ [$m^2$] and has been discretized with *384 x 128* collocation points. The cylinder has a diameter of *D=0,785* [*m*], with *64* lagrangian collocation points. The cylinder position in domain is shown in Fig. 4.

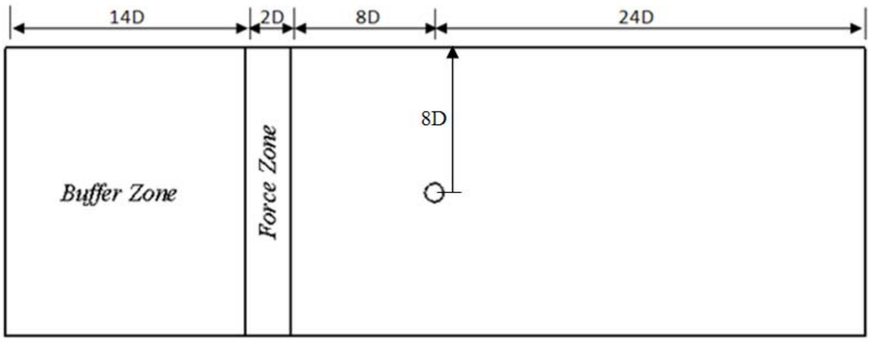


Figure 4. Calculus domain – circular cylinder.

At the top and bottom boundary conditions are periodicity. The inflow condition is a uniform profile of velocity ($U_\infty$=*1,0 m/s*). Other important parameter is the Reynolds number, that is *Re=100*, with the Reynolds number is possible to determine the viscosity of the fluid (equation 18):

$$\nu = \frac{U_\infty D}{\text{Re}} \qquad (22)$$

It also imposed a buffer zone:

$$ZA = \phi(Q_l - Qt_l) \qquad (23)$$

where *Q* is the problem solution, that is, *u* and v, *Qt* is the target solution, i.e. the solution is required in the final buffer zone, in this case, the target solution is an uniform profile $U_\infty$, and $\Phi$ is a parameter of stretching vortex, and it is calculated by Eq. (20):

$$\phi_\eta = \beta \left( \frac{x_\eta - x_{za}}{x_f - x_{za}} \right)^\alpha , \qquad (24)$$

where $\alpha$*=3.0* and $\beta$*=1.0* (UZUN, 2003), $x_{za}$ and $x_f$ are the beginning and the ending of buffer zone, respectively, $x_\eta$ is the generic position.

The force zone or porous medium is a range of thickness 2D, where is imposed the inflow profile by direct forcing, in order to aligned the streamlines. The Fig. 5 shows vorticity isocontours (*-1,0<w<1,0*) at time *t*=250*.

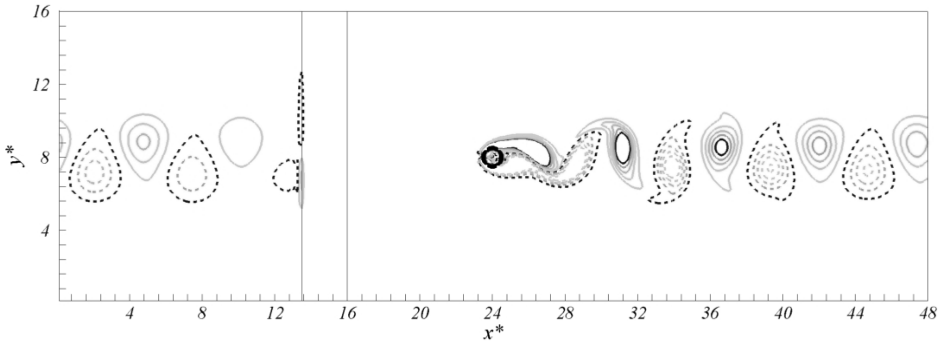


Figure 5. Isocontours of vorticity (-1,0<w<1,0) at *Re=100* in *t*=250*. - negative vortice; -- positive vorticity.

Fig. 6 shows a zoom at the region of immersed object and velocity vectors. It is possible seen the flow deviation of the obstacle and the flow inside the boundary, which arise for closing to divergent free.

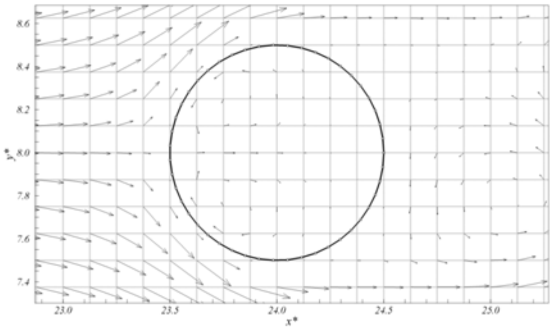


Figure 6. Velocity vectors at region of the immersed boundary.

Fig. 7 show the vorticity field for different simulation time steps.

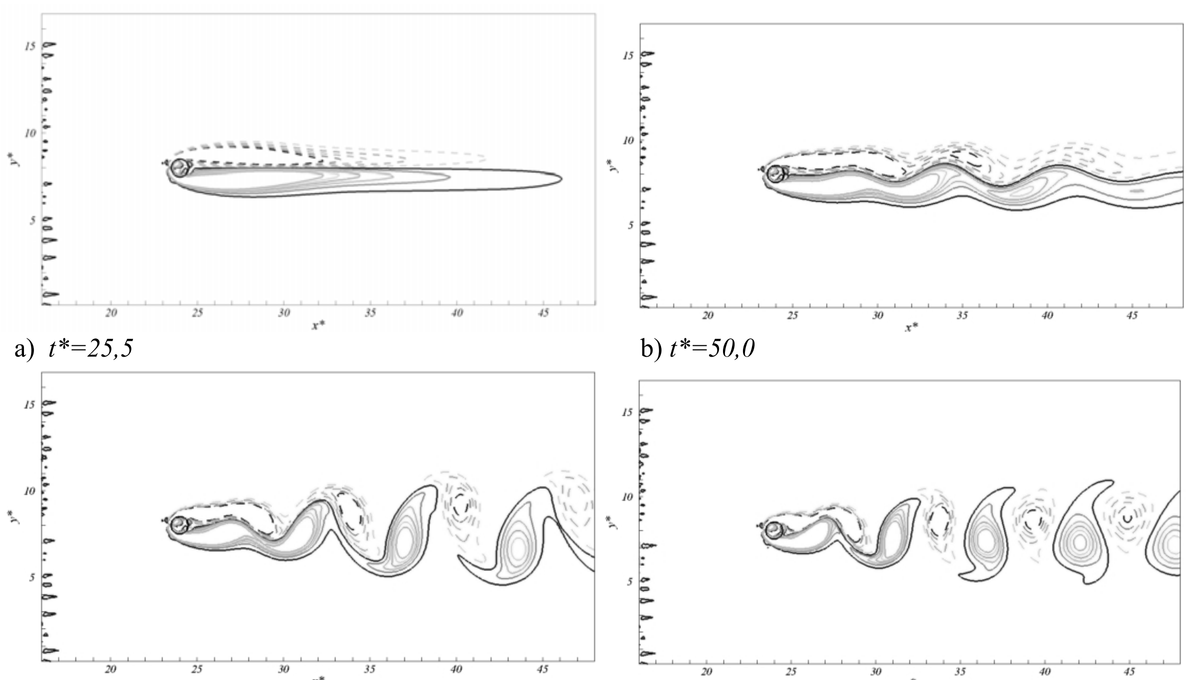

a) *t*=25,5*

b) *t*=50,0*

c) *t*=64,0*

d) *t*=89,0*

Figure 7. Temporal evolution of vorticity field at *Re=100*. - negative vortice; -- positive vorticity.

The first time at Fig. (7), in the beginning of simulation, arise two recirculation bubbles, in *t*=50* there is a formation of instability, and in the sequence appears the vortex shedding, *t*=64,0* and *t*=89,0*. Tab. 1, shows the comparison of Cd, Cl and St for different Reynolds numbers and among different authors.

Table 1. Comparison of drag coefficient and Strouhal number.

| | **Lima e Silva *et al.*(2003)** | | | **Lai and Peskin (2000)** | | | **Xu and Wang (2005)** | | | **Le, Khoo and Lin (2007)** | | | **Present work** | | |
|---|---|---|---|---|---|---|---|---|---|---|---|---|---|---|---|
| **Re** | *Cd* | *Cl* | *St* | *Cd* | *Cl* | *St* | *Cd* | *Cl* | *St* | *Cd* | *Cl* | *St* | *Cd* | *Cl* | *St* |
| 100 | 1,39 | 0,20 | 0,160 | 1,44 | 0,33 | 0,165 | 1,42 | 0,34 | 0,171 | 1,39 | 0,34 | 0,160 | 1,45 | 0,35 | 0,175 |
| 150 | 1,37 | 0,25 | 0,175 | 1,47 | 0,58 | 0,184 | | | | | | | 1,37 | 0,49 | 0,200 |
| 200 | | | | | | | 1,42 | 0,66 | 0,202 | 1,38 | 0,68 | 0,192 | 1,27 | 0,47 | 0,213 |
| 300 | 1,22 | 0,27 | 0,190 | | | | | | | | | | 1,08 | 0,39 | 0,221 |

Other important parameter of comparison is given by $L_2$ norm (equation 18) at the points of immersed boundary, rigorously, should be zero, but due numeric approaches, in this case, is not perfect and depends of Re. The accuracy of results is order $10^{-2}$, for more high Re.

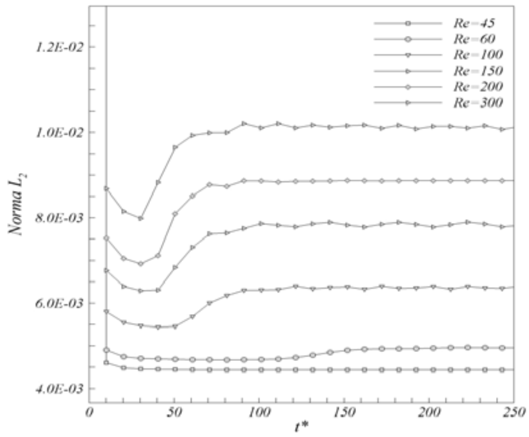


Figure 8. Temporal evolution of $L_2$ norm for different Reynolds numbers.

## 5. CONCLUSIONS

The motivations of this paper are improved the pseudo-spectral methodology, that is high order method and low computational cost, but restrained to periodic boundary conditions. Looking forward this aim a fusion of immersed boundary and the classic Fourier pseudo-spectral method was made.

The Fourier pseudo-spectral method allows solves the incompressible Navier-Stokes equations with the high order accuracy. In case where the equations to be solved are periodic the methodology accuracy order is high. It is observed in Taylor-Green flows in comparison between the analytical and numerical solution. Other great vantage is the computational cost when compared another high order methods, because the pressure disentail and the use FFT algorithm.

In the simulations of flowing over a circular cylinder it is possible to observe the drag and lift coefficients, and Sthrouhal number similar to another authors, and the vortex shedding are reasonable. The disadvantages are the requirement of using the buffer zone and the accuracy of methodology Fourier pseudo-spectral is penalized, but the computational cost is still low.

## 6. ACKNOWLEDGEMENTS

The authors thank the College of Engineering Mechanical (FEMEC) of the University Federal of the Uberlandia (UFU), Capes, CNPq and FAPEMIG to support.

## 7. REFERENCES

Briggs W.L. and Henson, V.E., 1995 “The DFT”, SIAM.

Canuto, C.; Hussaini, M.Y.; Quarteroni, A.; Zang, T.A. Spectral methods: fundamentals in single domains. New York: Springer-Verlag, 2006. 563p.

Canuto, C.; Hussaini, M.Y.; Quarteroni, A.; Zang, T.A. Spectral methods: evolution to complex geometries and applications to fluid dynamics. New York: Springer-Verlag, 2007. 596p.

Cooley, T.W. and Tukey, J.W., 1965 “An algorithm for the machine calculation of complex Fourier series”. Mathematics Computation. Vol. 19, pp. 297-301.

Peskin, C.S., 1972. “Flow patterns around heart valves: a numerical method”. Journal of Computational Physics, New York. Vol. 10, pp. 252-271.

Enriquez-Remigio, S. and Silveira-Neto, A. A new modeling of fluid-structure interaction problems through immersed boundary method/virtual psysical model (IBM/VPM). In: CONGRESSO BRASILEIRO DE ENGENHEIRA MECÂNICA, 19., 2007, Brasília. Anais... Brasília: ABCM, 2007. 1CD-ROM.

Goldstein, D., Adachi, T. and Sakata, H., 1993. “Modeling a no-slip flow with an external force field”. Journal Computational Physics, New York. v. 105, pp. 354.

Griffith, B. E.; Peskin, C. S. On the order of accuracy of the immersed boundary method: Higher order convergence rates for sufficiently smooth problems. Journal Computational Physics, New York, v. 208, p. 75-105, 2005.

Kim, J.; Kim, D.; Choi H. An immersed-boundary finite-volume method for simulations of flow in complex geometries. Journal of Computational Physics, New York, v. 171, p. 132-150, 2001.

Lai M. C.; Peskin, C. S. An immersed boundary method with formal second order accuracy and reduced numerical viscosity. Journal of Computational Physics, New York, v. 160, p. 705–719, 2000.

Le, D. V.; Khoo, B. C.; Lim, K. M. An implicit-forcing immersed boundary method for simulating viscous flows in irregular domains. Computer Methods in Applied Mechanics and Engineering, New York, v. 197, p. 2119-2130, 2008.

Lima e Silva, A., Silveira-Neto, A., and Damasceno, J., 2003. "Numerical simulation of two dimensional flows over a circular cylinder using the immersed boundary method", Journal of Computational Physics, New York. Vol. 189, pp. 351–370.

Mariano, F.P., 2007. "Simulação de escoamentos não periódicos utilizando as metodologias pseudo-espectral de Fourier e da fronteira imersa acopladas". 119 f. Dissertação (Mestrado em Engenharia Mecânica) – Faculdade de Engenharia Mecânica, Universidade Federal de Uberlândia.

Souza, A.M., 2005. "Análise numérica da transição à turbulência em escoamentos de jatos circulares livres". 180 f. Tese. (Doutorado em Mecânica) - Faculdade de Engenharia Mecânica, Universidade Federal de Uberlândia.

Uhlmann, M. An immersed boundary method with direct forcing for the simulation of particulate flows. Journal of Computational Physics, New York, v. 209, p. 448-476, 2005.

Uzun, A. 3-D Large-eddy simulation for jet aeroacoustics. 2003. 233 f. Tese (Doutorado em Engenharia Mecânica) - Purdue University, Pardue, 2003.

Wang Z.; Fan J.; Luo, K. Combined multi-direct forcing and immersed boundary method for simulating flows with moving particles. International Journal of Multiphase Flow, New York, v. 34, p. 283-302, 2008.

Xu, S.; Wang, Z. J. An immersed interface method for simulating the interaction of a fluid with moving boundaries. Journal of Computational Physics, New York, v. 216, p. 454-493, 2006.

## 8. RESPONSIBILITY NOTICE

The authors are the only responsible for the printed material included in this paper.